Journal of Materials Chemistry A

PAPER

View Article Online
View Journal | View Issue

Cite this: J. Mater. Chem. A, 2014, 2, 11966

Hierarchical architectures of monodisperse porous Cu microspheres: synthesis, growth mechanism, high-efficiency and recyclable catalytic performance†

Yu Zhang,[abc] Pengli Zhu,*[a] Liang Chen,[a] Gang Li,[a] Fengrui Zhou,[a] Daoqiang (Daniel) Lu,*[a] Rong Sun,*[a] Feng Zhou[b] and Ching-ping Wong[de]

Received 18th April 2014
Accepted 29th May 2014

DOI: 10.1039/c4ta01920b

www.rsc.org/MaterialsA

Novel hierarchical architectures of porous copper (Cu) microspheres assembled with nanoparticles have been successfully synthesized by ingeniously selecting the precursor and complexant through a facile wet chemical reduction method. The resultant porous Cu microspheres have a size distribution of 700 ± 50 nm and have excellent monodispersity. The synergistic effect between the precursor of slightly soluble copper hydroxide and the complexants of polyacrylic acid and ethanol amine exactly induces the generation of unique porous hierarchical architectures. The obtained porous Cu microspheres were applied to reduce and degrade different organic dyes with high concentrations (4-nitrophenol, methylene blue, and rhodamine B) in the presence of $NaBH_4$. Compared with solid Cu particles that have the same size, these porous Cu microspheres exhibit more excellent catalytic activity due to their hierarchical structures. Moreover, the catalyst with universal applicability could be easily separated from the catalytic system and sustainedly possess high stability in recycled reactions.

1 Introduction

Dyes are known as a major class of synthetic organic compounds released by many industries such as paper, plastic, leather, food, and textiles.[1,2] However, a vast majority of them are recognized as potential carcinogens that may also result in significant environmental pollution.[3] Nevertheless, most of these organic dyes are difficult to degrade unless in the presence of a catalyst. Photocatalysis,[4] metal catalysis[5,6] and microbial catalysis[1] are frequently used for dye degradation. Among them, metal particles such as Pt, Au, Ag, and Cu, which possess high catalytic activity and operability, are commonly used as catalysts for the reduction and degradation of organic dyes.[7–9]

In general, the catalytic properties of metal particles are a function of their morphology, size, and properties of carrier systems. Up to now, metal particles with various morphologies, including nanocubes,[10] nanorods,[11] nanoparticles,[12] nanodisks,[13] dendrites,[14] nanoclusters[5,15] and 3D hierarchical architectures,[6,16] have been synthesized by a variety of technologies. Among the aforementioned morphologies, widely used nanoparticles have been found to possess a more active catalytic effect due to their large specific surface area.[3,17] However, such nanoparticles usually need suitable support to prevent their aggregation during catalytic reactions. For applications taking place at low temperatures and in an aqueous environment, polymers,[9] gels,[17] and fibers[18] have been used as carrier substrates for these catalytic metal nanoparticles. Thus, the quantization, separation and reuse of catalysts based on metal nanoparticles with a smaller size are difficult, which also limits their practical applications. Therefore, hierarchical architecture porous metal microspheres composed of nanocrystallites might be one of the ideal structures for metal catalysts, which would possess a high specific surface area, large amount of catalytic sites, easy separability, and outstanding catalytic activity.

To date, porous metal materials like Au,[19] Pt,[20] Ag[21] and Ni[22] have been successfully prepared by chemical vapor deposition,[23] electrochemical method,[24,25] chemical etching method,[26] and template method.[27] However, there are only a few reports on the synthesis of porous Cu with hierarchical architectures. Hu and co-workers produced hierarchical porous copper dendrites by a facile hydrothermal treatment of a copper glycine complex in solution.[28] Porous cubic Cu microparticles with a good catalytic

[a]Shenzhen Institutes of Advanced Technology, Chinese Academy of Sciences, Shenzhen, China. E-mail: pl.zhu@siat.ac.cn; rong.sun@siat.ac.cn

[b]State Key Laboratory of Solid Lubrication Lanzhou Institute of Chemical Physics, Chinese Academy of Sciences, Lanzhou, China

[c]University of Chinese Academy of Sciences, Beijing, China

[d]School of Materials Science and Engineering, Georgia Institute of Technology, Atlanta, USA

[e]Department of Electronic Engineering, The Chinese University of Hong Kong, Hong Kong, China

† Electronic supplementary information (ESI) available: BET and TG figures, SEM images of contrast experiment results, UV spectra of three dyes degraded by $NaBH_4$ at three different conditions, stability test results of degrading MB and RhB with porous Cu microspheres. See DOI: 10.1039/c4ta01920b

performance were synthesized by a facile solvothermal method.[6] Despite these proven successes in growing porous metal materials, developing simple and low-cost synthetic technologies to fabricate porous Cu still remains a long-term challenge.

Herein, we report a facile aqueous-phase synthetic route of hierarchical porous Cu microspheres with an average size of 700 nm. The synthesis involves the reduction of copper hydroxide in the presence of hydrazine hydrate with poly(acrylic acid) and ethanol amine as complexing agents. Moreover, we propose the possible growth mechanism of porous Cu microspheres by monitoring and analyzing the products at various time intervals in combination with SEM and XRD characterizations. Because of their unique hierarchical architectures, these porous Cu microspheres are employed in the catalytic degradation of several organic dyes, including 4-nitrophenol, methylene blue and rhodamine B. In contrast to the solid Cu particles of equal size, the as-synthesized hierarchical architectures of porous Cu microspheres show much better catalytic efficiency and recyclability.

2 Experimental

2.1 Materials

Copper hydroxide and copper chloride were purchased from Aladdin Reagent Co., Ltd. Polyacrylic acid (PAA) aqueous solution (mass fraction of 50%), ethanol amine (EA), hydrazine hydrate (mass fraction of 85%), *p*-nitrophenol (4-NP, $C_6H_5NO_3$), methylene blue (MB, $C_{16}H_{18}ClN_3S$), rhodamine B (RhB, $C_{28}H_{31}ClN_2O_3$), and sodium borohydride were purchased from Sinopharm Chemical Reagent Co. Ltd. (China). Deionized water was used in all the experiments.

2.2 Preparation of porous Cu microspheres

In the typical preparation process, $Cu(OH)_2$ aqueous solution was prepared by dissolving 5 g $Cu(OH)_2$ and 5 mL PAA in 80 mL deionized water. After stirring for 20 min, 5 mL ethanol amine and 10 mL hydrazine hydrate were sequentially added to the blue reaction liquid. After continuing the reaction for an hour at room temperature, the colour of the system gradually changed from blue to khaki and then to reddish brown. The resultant dispersion was washed three times with ethanol and then water at 5000 rpm for 8 min *via* centrifugation. Finally, the products were dried at room temperature. Contrast experiments under the same procedures without PAA or by changing the precursor to $CuCl_2$ were also carried out.

2.3 Characterization

The characterizations of the samples were carried out by different techniques. The morphology and size of the synthesized porous Cu microspheres were observed with field-emission scanning electron microscope (FE-SEM, FEI Nova Nano SEM 450) and transmission electron microscope (TEM, FEI Tecnai G2F20S-TWIN). The Brunauer–Emmett–Teller (BET) surface area was determined by nitrogen adsorption and desorption using a specific surface area analyser (Micromeritics ASAP 2020, USA). The powder X-ray diffraction (XRD) patterns were recorded on an X-ray diffractometer (Rigaku D/Max 2500, Japan) with monochromated Cu-Kα radiation ($\lambda = 1.54$ Å). The ultraviolet-visible spectroscopy (UV-Vis) absorption spectra of the samples were recorded using a UV-Vis-NIR spectrometer (Shimadzu UV-3600, Japan) with a wavelength range of 250–800 nm. Thermogravimetry (TG) analysis was carried out with a thermogravimetric analyzer (TA Q600, Germany). All the measurements were performed at room temperature.

2.4 Evaluation of catalytic activity

The catalytic performance of the prepared porous Cu microspheres was determined by measuring the reduction and degradation of high concentration dyes in the presence of $NaBH_4$. Three typical dyes, namely, 4-NP, MB, and RhB, were selected as the degradation target molecules. Moreover, to evaluate the catalytic activity of the prepared porous Cu microspheres, we measured the reduction rates of different dyes with no Cu catalyst or catalyst with nearly the same size solid Cu spheres synthesized using the modified polyol method[12] described in our previous work.

In a typical activity test process, 5 mg Cu microspheres were dispersed into 5 mL deionized water. After ultrasonic dispersion, only 0.5 mL Cu solution was added to 30 mL 4-NP aqueous solution (0.2 mM), followed by the addition of 10 mL freshly prepared $NaBH_4$ solution (25 mM). Time-dependent absorption spectra during the catalytic reduction of dyes were recorded using a UV-Vis-NIR spectrophotometer by placing 2.5 mL of the sample solution into a 3 mL quartz cell. The catalytic degradations of the other two dyes were monitored under the same procedures. All the catalytic reactions were carried out at room temperature.

3 Results and discussion

3.1 Characterizations of porous Cu particles

Scanning electron microscopy and transmission electron microscopy were used to investigate the morphology and size of the synthesized porous Cu microspheres. Fig. 1 presents the typical SEM and TEM images of the products at different magnifications. As shown in the low magnification SEM image (Fig. 1a), the hierarchical microspheres with superior monodispersity and dispersion have a particle size distribution of 700 $\pm$ 50 nm. Moreover, the magnified SEM image reveals that the porous Cu microspheres exhibit a typical three-dimensional porous structure with a really rough surface (Fig. 1b). The uniform spherical building blocks (30 nm) mutually aggregated to create the whole hierarchical architecture. Furthermore, it is clear to observe that pores with a size of 80 nm are evenly distributed on the surface of the Cu microspheres. The TEM images at different magnifications of the prepared porous Cu microspheres are depicted in Fig. 1(c–e). From these images, it can be seen that the uniform hierarchical Cu microspheres are composed of small nanosized units. The diverse contrast in different positions similarly reflects the pores in the hierarchical porous microspheres. Next, the clear lattice fringes

marked by the white lines and the measured lattice *d*-spacing are 0.2103 nm and 0.2094 nm, respectively, which are very consistent with the interplane distance values of (111) in face-centered cubic Cu crystal (0.2088 nm). The BET surface area of the synthesized porous Cu microspheres and solid Cu spheres are 5.4 $m^2 g^{-1}$ and 1.7 $m^2 g^{-1}$ (Fig. S1†), further demonstrating the larger surface area of the porous Cu microspheres, which can be mainly attributed to the presence of pores on the surface.

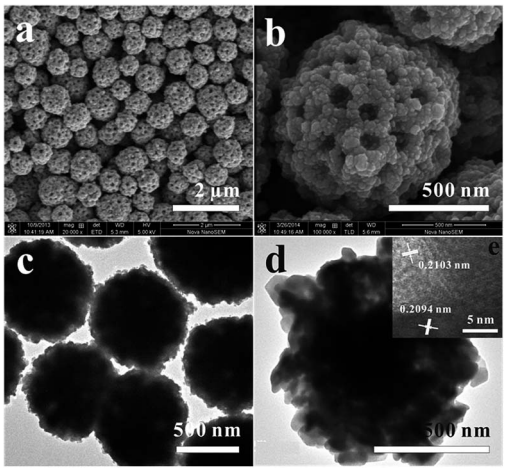

Fig. 1 SEM images (a and b) and TEM images (c–e) of the as-prepared porous Cu microspheres.

Fig. 2a shows the XRD pattern of the freshly produced microspheres. The diffraction peaks at 43.47°, 50.67° and 74.68° are attributed to the (111), (200) and (220) facets of the face-centered cubic (fcc) crystal structure. Hence, the as-prepared microspheres are confirmed to be phase-pure Cu (JCPDS no. 04-0836) without any impurity phases such as Cu_2O, CuO or $Cu(OH)_2$. It is well known that Cu is vulnerable to oxidation in atmospheric environment, which may limit its practical applications. Thus, in order to study the anti-oxidative ability of synthesized porous Cu microspheres, the XRD characterization was also performed on the same samples after being placed for

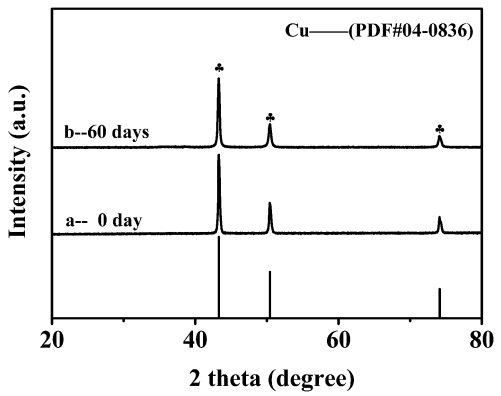

Fig. 2 XRD patterns of synthesized porous Cu microspheres: (a) freshly produced; (b) stored after 60 days.

60 days at room temperature under atmospheric pressure without strict conditions like nitrogen protection, the results of which are shown in Fig. 2b. It can be seen that the XRD pattern of the porous Cu microspheres stored for 60 days exhibits almost the same characteristic peak as the freshly produced particles. Moreover, no characteristic peaks of oxide impurities could be detected. This suggests that the synthesized porous Cu microspheres could be steadily placed for more than two months under ambient conditions, and even then exhibit strong oxidation resistance. Such strong oxidation resistance might be due to a protective agent coated on the particle surface. Thus, in order to confirm if there is a redundant complexant residue in the generated porous structure, TG analysis was performed from RT to 800 °C at the rate of 10 °C min^{-1} under a nitrogen flow (Fig. S2†). A thermal weight loss of 0.24% before 120 °C might be due to the adsorption of water on the sample. Moreover, the rest of the weight loss is about 2.16%, which could be attributed to the marginal amounts of PAA and EA adsorbed on the surface of the Cu microspheres. Combined with the XRD results, such a minute quantity of the protective agent layer not only largely improved the oxidation resistance of the hierarchical porous Cu microspheres, but also provided the necessary condition for their future applications.

3.2 Possible growth mechanism of porous Cu microspheres

For the purpose of explaining the formation process of the hierarchical porous Cu architectures, time-dependent experiments were carried out while the corresponding samples were collected at different time intervals from the reaction mixture. Fig. 3 shows the changes in the morphology of the samples, and Fig. 4 displays their corresponding XRD patterns. It can be seen that samples collected at 10 min have a size of 80–120 nm with

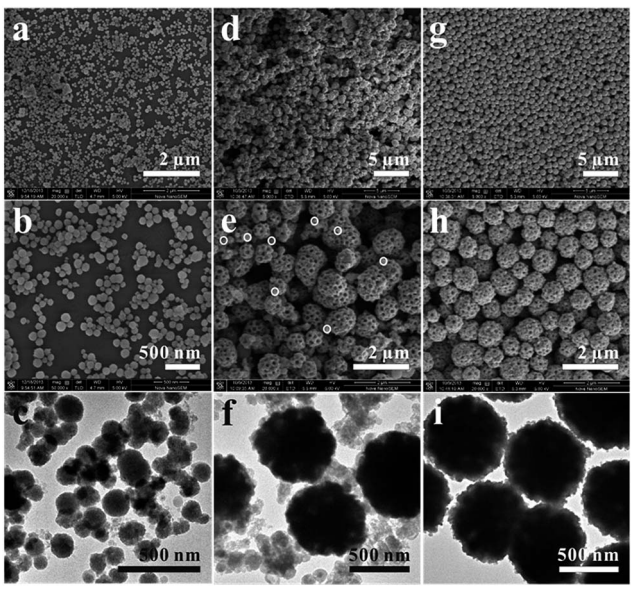

Fig. 3 SEM (a, b, d, e, g, and h) and TEM (c, f, and i) images of the process of hierarchical porous Cu architecture formation at different time intervals: (a–c) 10 min; (d–f) 30 min; (g–i) 60 min.

good monodispersity and smooth surface (Fig. 3a–c): the XRD pattern reveals that it is pure cuprous oxide (Fig. 4a). Then, as the reaction proceeds, spherical cuprous oxide nanoparticles gradually disappear accompanied with the formation of hierarchical porous structures (Fig. 3d–f). From the highly magnified image, it can be seen that the samples contain both smooth solid nanoparticles (circled in Fig. 3e) and hierarchical porous microspheres. Likewise, the corresponding XRD pattern (Fig. 4b) shows that the peaks belonging to copper are observed, which indicates that the samples obtained at this stage are a mixture of Cu and cuprous oxide. Finally, when the reaction time is prolonged to 60 min, spherical solid nanoparticles disappear and are completely transformed into uniform monodisperse porous Cu microspheres (Fig. 3g–i). Associated with the XRD pattern (Fig. 4c), the hierarchical porous structures are demonstrated to be phase-pure Cu without any impurity phases.

From the results of the above investigations, we propose a possible growth mechanism of the porous Cu microspheres, which is illustrated in Fig. 5. First, after adding PAA into the reaction solution, a small amount of Cu^{2+} is ionized from the $Cu(OH)_2$ dissolved in the weak acid aqueous solution. Cu^{2+} is then chelated with the carboxyl groups along the PAA chains and the PAA–Cu^{2+} complex is formed. Second, the addition of EA not only makes the complex compound of copper ions more stable, but also completes the requirement of an alkaline environment for the subsequent reduction reaction, in which the copper ions bonded on the PAA chains are reduced by hydrazine hydrate and *in situ* transformed to Cu_2O nanoparticles. Then, the initially formed Cu_2O nanoparticles are gradually reduced to elemental Cu. Moreover, the acting force of the carbonyl oxygen of PAA and elemental Cu cause the local collapse and condensation of polyacrylic acid chains so as to induce a cage effect. This prompts the adjacent Cu nanoparticles to gather into the hierarchical porous architectures. Furthermore, a large amount of N_2 microbubbles are released during the reaction, which might act as the soft templates of the pores. Finally, these factors together induced the formation of hierarchical porous Cu architectures.

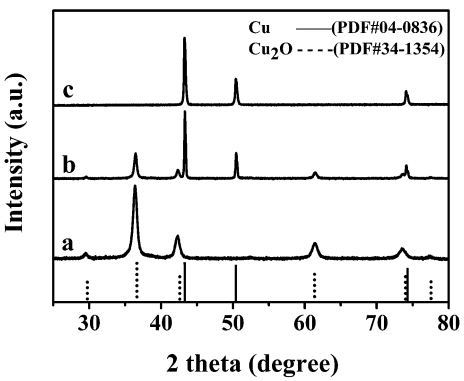

Fig. 4 XRD patterns of samples grown at different reaction times: (a) 10 min; (b) 30 min; (c) 60 min.

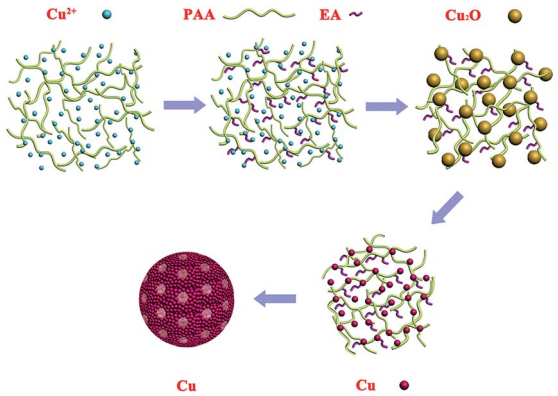

Fig. 5 Schematic illustration of the fabrication of hierarchical porous Cu microspheres.

In terms of controlling the experimental conditions, the preferred option of precursors and complexants both play vital roles in the generation of hierarchical architectures. First of all, the effect of the slightly soluble properties of copper hydroxide on the formation of porous structures could not be ignored. When soluble copper chloride was employed as the precursor, the resultant Cu particles were irregular (Fig. S3†). This reason might be explained as follows: when using a soluble copper source, there exists a large amount of Cu^{2+} in the reaction mixture; moreover, after adding PAA, numerous Cu^{2+} are bonded to the PAA chains and then transformed into bigger particles, which easily settled down in the system due to the excess nuclei centers. In the meantime, polyacrylic acid, an anionic water-soluble polymer electrolyte with good solubility in an aqueous solution, has been extensively selected as a modifier or template for the synthetic process of porous structures because it possesses a strong interaction effect and hydrophilic carbonyl groups.[29] Furthermore, it could not only provide steric hindrance to prevent the particles from aggregation, but also improve cross-linkage through the coordination and charge-attraction between the carboxyl and copper ions. Subsequently, a three-dimensional porous architecture could be formed due to the cross-linking of these colloidal particles. By means of the contrast experiments that were conducted without PAA (Fig. S4†), instead of porous Cu microspheres, only aggregated particles were obtained. Hence, in this cost-effective and easy-to-operate system, the slow ionization of cupric hydroxide, complexation of polyacrylic acid and ethanol amine, and strong reducibility of hydrazine hydrate together make it possible to synthesize monodisperse porous Cu microspheres.

3.3 Catalytic performances of prepared porous Cu microspheres

For the purpose of verifying its catalytic effect, the reduction rates of organic dyes by $NaBH_4$ were detected under three different conditions: without catalyst, in the presence of solid Cu particles, and porous Cu microspheres having the same size. The relative absorbance of dyes is plotted as a function of time to evaluate the reduction reaction rate. In the contrast

experiment, the solid Cu particles were synthesized by modified polyol method, and their morphology is shown in Fig. S5.†

4-NP is one of the most common organic pollutants in industrial waste waters, while its reduced form 4-aminophenol (4-AP) is an important industrial intermediate for the manufacture of analgesic and antipyretic drugs.[15,17,18] The heterogeneous catalytic reduction of 4-NP to 4-AP is not only environmentally and industrially important, but also useful as a model reaction to investigate the catalytic activities of different catalysts. The spectral band of 4-NP is known to appear at 400 nm, corresponding to the 4-NP anions under alkaline conditions. When the reduction of 4-NP is initiated, the absorption peak at 400 nm gradually decreases in intensity along with the increase of a new absorption peak at 300 nm, indicating the formation of 4-AP.[30] Therefore, this reduction procedure can be feasibly monitored by time-dependent UV-Vis absorption spectra. Fig. 6a represents the time-dependent UV-Vis absorption spectra in the presence of synthesized porous Cu microspheres. It clearly shows that the intensity of the absorption peaks of 4-NP at 400 nm decreases quickly with increasing time and new peaks at 300 nm concomitantly appear. The conversion process in which 4-NP transforms into 4-AP lasts for less than 18 min. However, 4-NP cannot be reduced by $NaBH_4$ unassisted with a catalyst (Fig. S6a†). The intensity of the absorption peak at 400 nm is almost unchanged after 120 min only with $NaBH_4$. Even with the support of solid Cu particles with nearly equal size as the catalyst, the reaction rate is relatively slow, which should take as long as 26 min for the complete reduction (Fig. S6b†). Obviously, the results reveal that the synthesized catalyst accelerates the reaction to a large extent. That is to say, the hierarchical architectures of Cu microspheres undergo more efficient catalysis than solid Cu particles.

For the sake of examining the universality of the as-synthesized porous Cu microspheres as catalysts for the reduction and degradation of organic dyes, we also chose MB and RhB as the test targets. First, for MB, a heterocyclic aromatic water-soluble dye was selected, the catalytic degradation of which has been studied for years. The UV-Vis band of the MB monomer in an aqueous medium appears normally at 665 nm, corresponding to the n–π* transition and a shoulder peak at 614 nm.[31–33] The decreasing trend of the absorption intensity in a regular interval of time (15 min) indicates the degradation of MB to leucomethylene blue (LMB) by $NaBH_4$ without a catalyst, but at an extremely slow pace (Fig. S7a†). Then, the plot of the relative absorption intensity with a time-interval of 2 min reveals that the degradation of MB by $NaBH_4$ supported with solid Cu particles proceeds for a period of 12 min (Fig. S7b†). However, the complete degradation of MB to LMB is accomplished in less than 8 min in the presence of porous Cu microspheres (Fig. 6b or S7c†), namely, the degradation process is found to be further facilitated upon the incorporation of the prepared hierarchical Cu microspheres. The other target, RhB, is a type of synthetic dye with a fresh peach colour, which can be used as a fluorescence dye in the lab.[4,34] Fig. 6c shows a series of UV-visible absorption spectra of the degradation of RhB with the support of porous Cu microspheres. When the reduction of RhB is initiated, the spectral band of RhB at 553 nm rapidly decreases in intensity with increasing reaction time to almost zero within 4 min (Fig. 6c or S8c†). Yet, the reaction rate without a catalyst is much slower and takes as long as 45 min for the complete degradation (Fig. S8a†). Even after adding solid Cu particles as the catalyst, the degradation of RhB by $NaBH_4$ needs 6 min (Fig. S8b†). Then, the reaction kinetics of the degradation of the three organic dyes under different catalytic conditions are calculated separately by monitoring their time-dependent UV-Vis absorption spectra. In this catalytic reaction system, since the amount of reductant $NaBH_4$ is excessive compared to the degraded dyes (4-NP, MB, and RhB), the reaction rate is roughly independent of the $NaBH_4$ concentration, and the kinetics can be considered pseudo-first-order with respect to the dyes only.[17,35,36] Hence, the reaction kinetics can be described as $\ln(A/A_0) = -kt$, where k is the apparent first-order rate constant (min^{-1}) and t is the reaction time (min).[37] Here, A and A_0 are the absorbances of the dyes at time t and 0, respectively, which are proportional to the real-time concentrations. Therefore, we plot $\ln(A/A_0)$ against the reaction time t and the results are shown in Fig. 7. It indicates that $\ln(A/A_0)$ exhibits good linear correlation with the reaction time under three different conditions, confirming that the reductions and degradations of the three kinds of organic dyes follow the pseudo-first-order kinetics. The apparent reaction rate constant k could be directly obtained from the slope of the linear plots. For the first dye (4-NP), we can obviously determine that the value of k without a catalyst is low (0.00015), intuitively reflecting that the degradation of 4-NP only

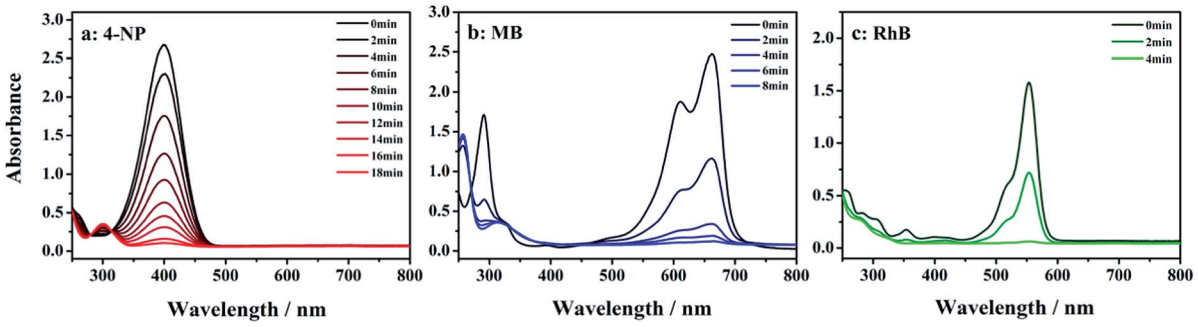

Fig. 6 UV-visible absorption spectra of catalytic degradation of (a) 4-NP; (b) MB; and (c) RhB by $NaBH_4$ with synthesized porous Cu microspheres.

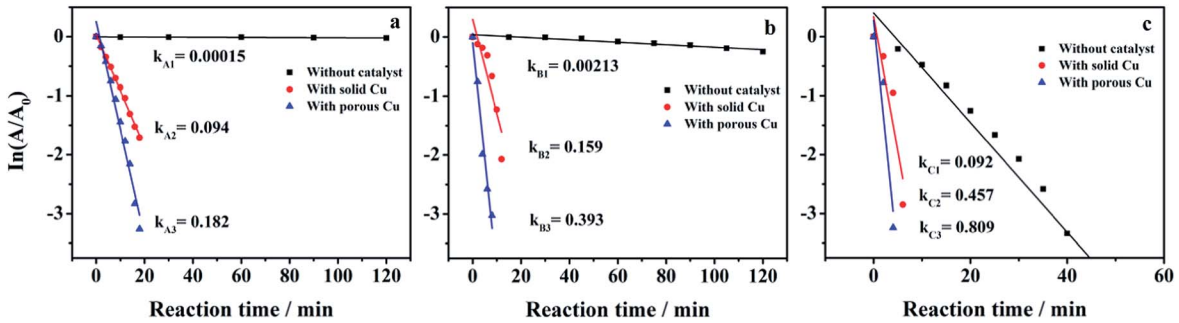

Fig. 7 Plots of $\ln(A/A_0)$ against the reaction time t for (a) 4-NP; (b) MB; (c) RhB.

with $NaBH_4$ is difficult. Then, the rate constant k increases up to 0.094 with solid Cu particles as the catalyst, which indicates a catalytic effect. Moreover, for the catalytic system supported with the as-synthesized porous Cu microspheres, the value of k is 0.182, which is almost twice that of the system assisted with solid Cu particles. The increase of the rate constant directly indicates the speeding up of the degradation of the dye. As for the other two kinds of dyes, the values of the rate constant k with the porous Cu microspheres are both nearly doubled compared with those using solid Cu particles, which proves that the prepared porous Cu microspheres exhibit high-efficiency catalytic activity for diversiform dyes as that indicated in the previous results.

The main reason for the excellent catalytic activity of the synthesized porous Cu microspheres is associated with their special structure. Metal particles are capable of catalysing the reduction and degradation reactions owing to their ability of assisting the electron relay from the donor to the acceptor.[38,39] The particles that possess large surface areas might act as good substrates for the electron transfer reaction. Catalysis occurs only on the surface of metal particles; therefore, increasing the available surface area will greatly enhance the effectiveness of the catalyst. As mentioned above, the as-prepared catalyst owns hierarchical porous architectures and its surface is rather rough, with many small pores evenly distributed on the surface (Fig. 8).

The large specific area of the nanoparticles-assembled porous structure increases the catalytic reactivity to a large extent. The reducing agent adsorbed on the surface of porous Cu microspheres may also promote the catalytic degradation. Hence, the oxidation-reduction between the active dyes and $NaBH_4$ could happen more easily, effectively and faster under the catalysis of porous Cu microspheres.

The porous microspheres consist of densely crowded Cu nanoparticles with a size of several tens of nanometers. In other words, compared with nanoparticles, the porous Cu microspheres have the merits of less aggregation during the catalytic process, and also the catalyst could be easily separated from the reaction medium due to their micrometer size and may be reused after washing with distilled water. In order to evaluate the stability and recyclability of the porous Cu catalyst in degradation dyes, the successive cycles of catalytic 4-NP are explored, and the results are shown in Fig. 9. In the first two cycles, the degradation rates are 100%, indicating the complete degradation of 4-NP. With the increase in cycling times, the degradation rates drop only marginally; moreover, till the sixth cycle, the degradation rate of 4-NP remains at about 90%, indicating the high stability of porous Cu microspheres in dye degradation reactions. Furthermore, recycling experiments involving the other two dyes were also carried out, and till the sixth cycle, the degradation rates of both MB and RhB were maintained higher than 94% (Fig. S9a and b†). On the whole, these kinds of hierarchical porous Cu microspheres exhibit not only high catalytic efficiency but also good stability and

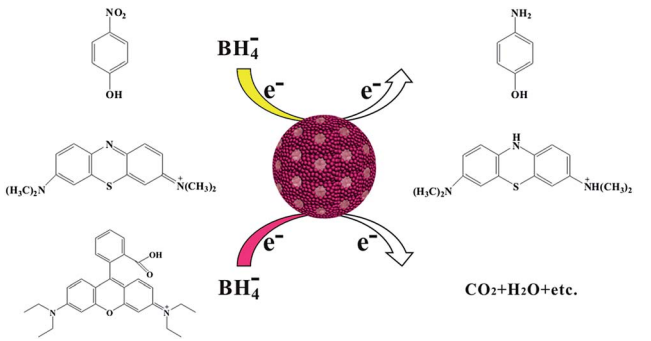

Fig. 8 Mechanism of the catalytic reduction and degradation of dyes with porous Cu microspheres.

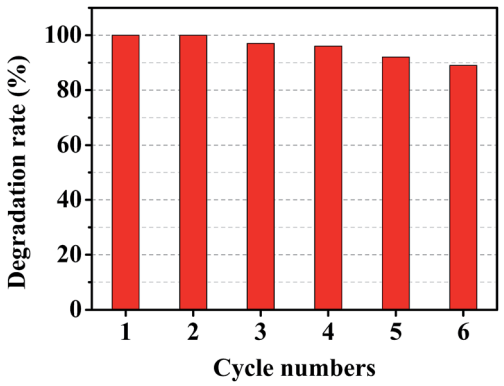

Fig. 9 Stability test of the prepared hierarchical porous Cu microspheres in reduction of 4-NP.

recyclability in different organic dye degradation reactions, which promote their practical applications.

4 Conclusions

Porous Cu microspheres with hierarchical architectures have been successfully synthesized by a facile chemical reduction method in an aqueous medium. The obtained nanoparticle-assembled Cu microspheres have an average size of 700 ± 50 nm with high monodispersity, purity and anti-oxidation properties. In particular, the hierarchical porous Cu microspheres exhibit outstanding activity in the catalytic reduction and degradation of different organic dyes. Experimental results show that the rate constant k with the assistance of porous Cu particles is twice that obtained by the support of solid Cu particles. Moreover, the prepared porous Cu microspheres with extensive applicability could not only be easily separated from the catalytic reduction system, but also be recycled effectively. All these features make the obtained porous Cu microspheres not only reflect the excellent performance in terms of catalysis, but also promote their applications in other aspects of multi-functional materials such as antifogging, self-cleaning, anti-bacterial, stain-proofing agents, and cathode catalyst in alkaline fuel cells.

Acknowledgements

This work was financially supported by the National Basic Research Program of China (973 Program) (2012CB933700-G), National Natural Science Foundation of China (21101165), Guangdong Innovative Research Team Program (no. 2011D052 and KYPT20121228160843692), Shenzhen Electronic Packaging Materials Engineering Laboratory (2012-372), Shenzhen basic research plan (JC201005270372A, GJHS20120702091802836 and JSGG20120615161915279).

Notes and references

1 I. M. Banat, P. Nigam, D. Singh and R. Marchant, *Bioresour. Technol.*, 1996, **58**, 217–227.
2 C. A. Martinez-Huitle and E. Brillas, *Appl. Catal., B*, 2009, **87**, 105–145.
3 V. K. Vidhu and D. Philip, *Micron*, 2014, **56**, 54–62.
4 J. T. Zhang, Z. G. Xiong and X. S. Zhao, *J. Mater. Chem.*, 2011, **21**, 3634–3640.
5 N. Vilar-Vidal, J. Rivas and M. A. Lopez-Quintela, *ACS Catal.*, 2012, **2**, 1693–1697.
6 Z. L. Zhang, H. W. Che, Y. L. Wang, X. L. She, J. Sun, P. Gunawan, Z. Y. Zhong and F. B. Su, *ACS Appl. Mater. Interfaces*, 2012, **4**, 1295–1302.
7 N. R. Jana, T. K. Sau and T. Pal, *J. Phys. Chem. B*, 1999, **103**, 115–121.
8 I. K. Sen, K. Maity and S. S. Islam, *Carbohydr. Polym.*, 2013, **91**, 518–528.
9 M. Dasog, W. Hou and R. W. J. Scott, *Chem. Commun.*, 2011, **47**, 8569–8571.
10 H. C. Gao, Y. X. Wang, F. Xiao, C. B. Ching and H. W. Duan, *J. Phys. Chem. C*, 2012, **116**, 7719–7725.
11 I. Lisiecki, A. Filankembo, H. Sack-Kongehl, K. Weiss, M. P. Pileni and J. Urban, *Phys. Rev. B: Condens. Matter Mater. Phys.*, 2000, **61**, 4968–4974.
12 Y. Zhang, P. L. Zhu, G. Li, T. Zhao, X. Z. Fu, R. Sun, F. Zhou and C. P. Wong, *ACS Appl. Mater. Interfaces*, 2014, **6**, 560–567.
13 C. Salzemann, J. Urban, I. Lisiecki and M. P. Pileni, *Adv. Funct. Mater.*, 2005, **15**, 1277–1284.
14 J. Liu, Q. Wu, F. L. Huang, H. F. Zhang, S. L. Xu, W. Huang and Z. L. Li, *RSC Adv.*, 2013, **3**, 14312–14321.
15 J. S. Shen, Y. L. Chen, Q. P. Wang, T. Yu, X. Y. Huang, Y. Yang and H. W. Zhang, *J. Mater. Chem. C*, 2013, **1**, 2092–2096.
16 C. C. Kong, S. D. Sun, J. Zhang, H. D. Zhao, X. P. Song and Z. M. Yang, *CrystEngComm*, 2012, **14**, 5737–5740.
17 L. H. Ai, H. T. Yue and J. Jiang, *J. Mater. Chem.*, 2012, **22**, 23447–23453.
18 P. Zhang, C. L. Shao, Z. Y. Zhang, M. Y. Zhang, J. B. Mu, Z. C. Guo and Y. C. Liu, *Nanoscale*, 2011, **3**, 3357–3363.
19 Q. F. Zhang, N. Large, P. Nordlander and H. Wang, *J. Phys. Chem. Lett.*, 2014, **5**, 370–374.
20 Z. R. Shen, Y. Matsuki, K. Higashimine, M. Miyake and T. Shimoda, *Chem. Lett.*, 2012, **41**, 644–646.
21 H. He, W. P. Cai, Z. F. Dai, G. Q. Liu and H. H. Li, *Nanotechnology*, 2013, **24**, 465302.
22 Z. J. Jiao, N. Takagi, N. Shikazono and N. Kasagi, *J. Power Sources*, 2011, **196**, 1019–1029.
23 X. D. Wang, C. J. Summers and Z. L. Wang, *Adv. Mater.*, 2004, **16**, 1215–1218.
24 C. Fang, A. V. Ellis and N. H. Voelcker, *J. Electroanal. Chem.*, 2011, **659**, 151–160.
25 D. Gloria, J. J. Gooding, G. Moran and D. B. Hibbert, *J. Electroanal. Chem.*, 2011, **656**, 114–119.
26 Y. Yang, Y. H. Wu, P. Hao and Z. Q. Zhang, *Spectrosc. Spectral Anal.*, 2010, **30**, 1898–1901.
27 Y. Li, W. Z. Jia, Y. Y. Song and X. H. Xia, *Chem. Mater.*, 2007, **19**, 5758–5764.
28 C. Q. Hu, Z. Gao and X. R. Yang, *J. Cryst. Growth*, 2007, **306**, 390–394.
29 Y. T. Bi, H. B. Ren, B. W. Chen, G. Chen, Y. Mei and L. Zhang, *J. Sol-Gel Sci. Technol.*, 2012, **63**, 140–145.
30 H. L. Jiang, T. Akita, T. Ishida, M. Haruta and Q. Xu, *J. Am. Chem. Soc.*, 2011, **133**, 1304–1306.
31 D. Heger, J. Jirkovsky and P. Klan, *J. Phys. Chem. A*, 2005, **109**, 6702–6709.
32 T. Shahwan, S. Abu Sirriah, M. Nairat, E. Boyaci, A. E. Eroglu, T. B. Scott and K. R. Hallam, *Chem. Eng. J.*, 2011, **172**, 258–266.
33 Y. G. Hu, T. Zhao, P. L. Zhu and R. Sun, *Colloid Polym. Sci.*, 2012, **290**, 401–409.
34 J. A. Kwak, D. K. Lee and D. J. Jang, *Appl. Catal., B*, 2013, **142**, 323–328.
35 S. Ghosh, S. Patil, M. Ahire, R. Kitture, D. D. Gurav, A. M. Jabgunde, S. Kale, K. Pardesi, V. Shinde, J. Bellare, D. D. Dhavale and B. A. Chopade, *J. Nanobiotechnol.*, 2012, **10**, 17.

36 Z. Y. Zhang, C. L. Shao, Y. Y. Sun, J. B. Mu, M. Y. Zhang, P. Zhang, Z. C. Guo, P. P. Liang, C. H. Wang and Y. C. Liu, *J. Mater. Chem.*, 2012, **22**, 1387–1395.
37 S. Y. Gao, X. X. Jia, J. M. Yang and X. J. Wei, *J. Mater. Chem.*, 2012, **22**, 21733–21739.
38 V. K. Vidhu and D. Philip, *Spectrochim. Acta, Part A*, 2014, **117**, 102–108.
39 H. Hu, M. W. Shao, W. Zhang, L. Lu, H. Wang and S. Wang, *J. Phys. Chem. C*, 2007, **111**, 3467–3470.